

Breakthrough Analysis of Empty Fruit Bunch-Based Hydrogel Biochar Composite (EFB-HBC) for Hydrogen Sulphide (H₂S) Adsorption Study Removal

Nik Muhammad Faisal Mat Yasin¹, Nor Hidayah Meri¹, Norhayati Talib¹, Wan Azlina Wan Abdul Karim Ghani², Zulkifli Abdul Rashid^{1,3}, Azil Bahari Alias^{*1,3}

¹Faculty of Chemical Engineering, Universiti Teknologi MARA, Selangor, Malaysia

²Department of Chemical & Environmental Engineering, Faculty of Engineering, Universiti Putra Malaysia, Selangor, Malaysia

³Centre of Industrial Process Reliability & Sustainability (INPRES), Faculty of Chemical Engineering, Universiti Teknologi MARA, Selangor, Malaysia

*Corresponding author: Azil Bahari Alias, email: azilbahari@uitm.edu.my

ABSTRACT

Hydrogen sulphide (H₂S) is always present in biogas, and causes odours, corrosiveness, and sulphur emissions when the gas is burned. It is used regularly in internal combustion engines, turbines or fuel cells, the removal of hydrogen sulphide from biogas is required to protect the equipment. More importantly, it causes respiratory complication when its concentration reaches above 50 ppm. Many technologies have been developed to remediate H₂S contamination in flue gas, among which biochar is one of the most sustainable and promising. However, the biochar low porosity is major challenge as good adsorbent. Therefore, highly porous and inexpensive acrylamide was used to synthesize polyacrylamide hydrogel-biochar composites using microwave pyrolyzed raw and treated Empty Fruit Bunch (EFB) biochars as precursor. The phenol treated EFB-HBC composites significantly improved the surface chemistry of the composite and hence the adsorption capacity. According to the breakthrough curves, the maximum the sorption performance of H₂S was optimum using a fine size of EFB-HBC highest adsorption capacity (102.9 mg/g) and breakthrough time of 85 minutes compared to other samples. Besides the greater swelling capacity, the significantly improved ability of HBC composite to entrap H₂S from gas media was hypothetically attributed to the formation of ionic attraction fields around scattered biochar particles.

Keywords: Empty fruit bunch, biochar, hydrogel biochar, sorption, hydrogen sulphide

1. INTRODUCTION

Hydrogen sulphide (H₂S) is always present in biogas, although concentrations vary with the feedstock. The concentration of hydrogen sulphide in the gas is a function of the digester feed substrate and inorganic sulphate content. Wastes which are high in proteins containing sulphur-based amino acids (methionine and cysteine) can significantly influence biogas hydrogen sulphide levels. Hydrogen sulphide (H₂S) in biogas causes odours, corrosiveness, and sulphur emissions when the gas is burned. Besides, H₂S can corrode and damage the equipment [1]. H₂S emission is extremely dangerous when the concentration of H₂S reaches up to over 50 ppm when released to the environment, and unconsciousness will occur within a few minutes along with respiratory paralysis, followed by death [2]. Several treatment methods like iron sponge, iron oxide pellets, activated carbon, water scrubbing, sodium hydroxide (NaOH) scrubbing, biological removal on a filter bed are used for hydrogen sulphide removal from biogas. Among these, adsorption technologies are preferable and parameters like adsorption capacity; labour requirements to do exchanges; disposal and

transport cost of waste is the priority considerations when developing the adsorbents. Activated carbon (AC) been used for many years for this gas removal as AC is mainly amorphous material that has large surface area and pore volume. However, in the removal of harmful gases such as H₂S which considered wet gases, absorption mechanism is essential to trap the water presence. Therefore, in this study Empty Fruit Bunch (EFB)-based hydrogel (EFB-HBC) composite was introduced to for simultaneous effect on water and gas removal H₂S from the gas stream.

The biomass generated at the mill from the processing of the 101.022 million tonnes of Fresh Fruit Bunch (FFB) harvested, about 23.24 million tonnes of EFB are generated [3]. Thus, EFB caused major disposal issue in palm oil plantation industry and hence conversion into value added products is necessary. Many studies reported that due to its high cellulose content this material can be the precursor to another usable material such as adsorbent [4]. Although EFB has high cellulose content, due to low surface area and pore volume it is not good adsorbent. Carbonization of raw EFB into biochar would increase carbon content and larger surface area and hence the adsorption capacity [5]. However, the combination with hydrophilic materials such as hydrogel that would absorb water presence in H₂S would

make it better. Hydrogels are also known as hydrophilic gels that are water-swollen, cross-linked polymeric structures containing either a covalent bond which is produced by a simple reaction of one or more than one monomer. Moreover, hydrogels can adsorb water without dissolving. Hydrogels are very soft, smart, and has a high capacity to adsorb water [6]. The ability of hydrogels to adsorb water arises from hydrophilic functional group attached to the polymer structure while their resistance to dissolutions from crosslinks between network chains. Hydrophilic explains that, water inside hydrogels allows free diffusion of solute molecules such dyes and heavy metals, while polymer serves as a matrix to hold water together [7]. Therefore, the combination of hydrogel and biochar will give a high impact on sorption results.

The application of HBC is considered as a new innovation and still in development studies. The combination of HBC and EFB will open new possibility in enhancing biomass structure and sorption. This research will focus on characterization of Empty Fruit Bunch (EFB)-based hydrogel (EFB-HBC) and adsorption breakthrough performance of H₂S on the effect of bed height. This research highlight differences on conditions of EFB-HBC in terms of dryness and sizes toward sorption.

2. EXPERIMENTAL

2.1 Raw Materials & Chemicals

Empty Fruit Bunch (EFB) has been chosen as the raw material and was obtained from one of the palm oil industries located in Banting, Selangor. Other chemicals for HBC synthesis are Acrylamide (AAM) as monomer, N,N'-methylenebisacrylamide (MBA) as cross-linker, and ammonium persulfate (APS) as initiator which is, supplied by R&M chemical.

2.2 Biochar Production

The microwave-assisted pyrolysis technique was applied in producing EFB biochar in this study. 200g of raw Empty Fruit Bunch (EFB) was placed in the quartz reactor in the microwave pyrolyzer at 1000 W of microwave power level for 30 minutes under nitrogen flow at 150 mL/min. The method to prepare EFB char by using microwave-assisted pyrolysis is referring to Zakiuddin Januri et al. (2014) with some modification [8].

2.3 Acid Washing Pre-treatment

Acid washing pre-treatment was carried out using Hydrochloric Acid (HCl) and Hydrogen Peroxide H₂O₂ [9-10]. Next, 2 L of diluted 0.1 M HCl and 0.1 M H₂O₂ solutions were prepared in a 2L volumetric flask as a stock chemical solution. Then 10g of EFB biochar was pre-treated with 200 mL of the prepared acid solution in a closed beaker

for 6 hrs. Finally, the biochar was washed with distilled water until a neutral pH is obtained and oven then dried at 80 °C overnight. The pre-treated biochars, biochar H100, and biochar P100 with HCl and H₂O₂ solutions respectively.

2.4 Hydrogel Biochar Production

EFB-HBC was synthesized using 1.0 g of AAM which was dissolved in 1.0 mL of distilled water. Then, 0.6 g of Empty Fruit Bunch (EFB) biochar and 0.001 g of MBA was added to the AAM solution. After thorough mixing, 0.2 mL of 0.1 g aqueous solution of APS was added to initiate the polymerization. The hydrogel biochar precursor solution was immediately placed into a plastic mold and placed in an oven at 40 °C for 30 mins. The plastic mold containing hydrogel biochar composites was removed from the oven after 30 min and left for 24 hrs at room temperature to ensure complete polymerization and crosslinking. EFB-HB was taken from the plastic mold, cut to desired sizes, and washed several times with distilled water to remove all unreacted monomers and low molecular weight polymeric matters from the hydrogel. The washed EFB-HB was first air-dried before drying in a vacuum oven at 40 °C for 24 hrs. This hydrogel formation method is following the procedure used by Karakoyun et al., (2011) with some alteration [11].

2.5 Physico-chemical Characterizations

Field Emission Scanning Electronic Microscopic (FESEM) model SUPRA 40VP was used to evaluate the morphology trend of pores on the surface of samples. FESEM operated at all accelerating voltage and the working distance used was 5kV and 5mm, respectively. Before proceeding with the FESEM analysis, all the samples were coated in gold to remove any residual ions on the samples. Then, the image was captured under magnification of 500X in 10 µm size. The Brunauer-Emmet-Teller (BET) theory was used to determine the surface area, pore volume and pore size distribution of xerogels. For this analysis, the low-temperature N₂ adsorption/desorption analysis was carried out to investigate the structural properties of the produced xerogels adsorbent. Experiments were performed at 77K and were degassed at 60°C under vacuum before analysis [12].

For the maximum temperature of samples and element content such as moisture content, volatile matter content, carbon content, and ash content, they were determined and analyzed by Thermogravimetry Analysis (TGA) under 10 °C/min of proximate gas with an initial mass of the sample is 20 mg.

DSC is a thermal analysis technique that shows the relation between material heat capacity changes by temperature or, in other words, it determines the heat required to increase the temperature of samples. This instrument was operated with a sample weight ranging 5 to 10 mg in powder form heating from 30°C to 300°C at a heating rate of 10°C/min [13].

Fourier Transform Infrared Spectroscopy (FTIR) will be used for measuring and analyzing the functional group of samples. This instrument can be applied to investigate structural changes of biochars as a function of different sample preparation (pre-treatment process). In this research, FTIR will be performed by using Perkin – Elmer Spectrum 2000 FTIR with a wavelength of 4000 – 600 cm^{-1} [14].

2.6 Sorption Test

The sorption experiment was carried out in a multilayer sorption column consisting of three layers of sorption trays as shown in Figure 1. The column was made of stainless steel due to corrosive gases were used. The inner diameter and each tray heights are 1.85 inches and 3 inches respectively. For every 1 inch of filter trays filled with glass wool to avoid the fine particles passing through the system and clogging the gas way. The filter trays were filled with total bed heights of 1.5inch, 3 inches, and 6 inches and the sorption experiment were performed by corresponding to the mass of granule size EFB-HBC 12g, 18g, and 36g. In addition, the fixed parameters used are 25 ppm inlet concentration, the gas flow 60 L/min controlled by a rotameter to the adsorption system, and the system was run at temperature 27°C. Finally, gas will pass through the outlet tube which was connected to the sensory system (Gasman H2S Detector). The next step is, the fine size of EFB-HBC was tested as sorbent with the same parameter, and the sorption performance was compared with the granule size of EFB-HBC.

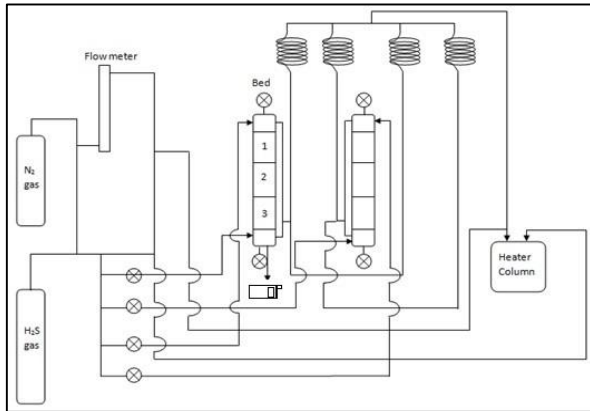


Figure 1 Multilayer adsorption system (detail labelling)

For further research, the idea to add some amount of water to EFB-HBC was triggered by a previous study. Based on White's (2010) studies, pressurized water is sprayed to the system while the biogas was injected into the sorption column to make an additional attraction between adsorbent and H_2S [15]. Then, with the special characterization of hydrogel which can store water, the water was added to EFB-HBC until the weight of the adsorbent became doubled. With the same parameters, wet granule and wet fine size of EFB-HBC were tested on sorption performance

and the results were compared. The result of sorption performance was interpreted by analyzing the breakthrough curves formed from the sorption process and the sorption capacity (mg/g) calculated from the area breakthrough curve by using a trapezoidal technique, as shown in Figure 2. In order to get accurate reading, sorption experiment was carried out three times and average out the readings. This method was used to remove parallax error that caused unintentional during sorption tests.

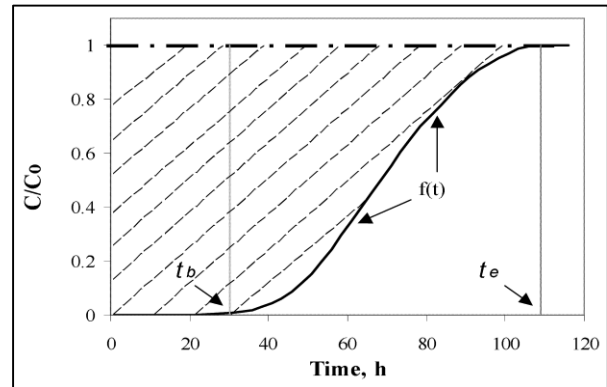


Figure 2 Area of breakthrough curve as adsorption capacity

3. RESULTS AND DISCUSSION

3.1 Physico-chemical characterizations

Figure 3 shows SEM image for all samples. It can be seen significant pore enlargement from raw EFB to biochar biochar (see Figure 3.a and 3.b). Due to the pore enlargement, Sadaka (2008) has explained in the pyrolysis process that components like cellulose, hemicellulose, and lignin were broken down to form low molecular weight of volatile products and at the same time, the pores become bigger [16]. In this study, H_2O_2 pre-treated biochar (Fig. 3-d) showed the significance improvement compared to HCL pre-treated biochar (Fig. 3-c) from this study pore The reason is that H_2O_2 is an oxidizing agent and one of alkaline peroxide which can remove partial lignin and form the hemicellulose wall has become thinner [17]. In comparison, EFB-HBC H100 (Fig. 3.e) has a thicker lignocellulose wall compared to EFB-HBC P100 (Fig. 3.f), and Gunawan et al., (2009) have claimed that this lignocellulosic fiber has characteristics such good tensile strength and strong cellulose backbone [7]. However, after polymerized the biochar became HBC, the lignocellulose wall grew stronger and was protected by the presence of cross-linker which evidently from EFB-HBC P100 which indicated the potential as adsorbent because the ability of adsorption will depend on the surface area and pore structure [18]. Table 1 shows the results of BET surface area, the total pore volume, and average pore size for all samples. EFB-HBC

P100 showed higher BET surface area and total pore volume with 1.5997 m²/g and 0.000965 cm³/g respectively while for EFB-HBC H100 it is 1.2562 m²/g and 0.000951 cm³/g. Based on Table 1, it showed that the average pore size of EFB-HBC P100 is 3.83805 nm which is higher compared to EFB-HB H100 3.0272 nm. Both HBCs are considered mesopore since the average pore size is in the

range of 2 to 50 nm which clustered as type II of BET shown on Figure 4 which indicates it is a uniform macropores and has strong interaction with the surface [19].

Figure 3 SEM Images (magnification of 500X in 10 μm size)

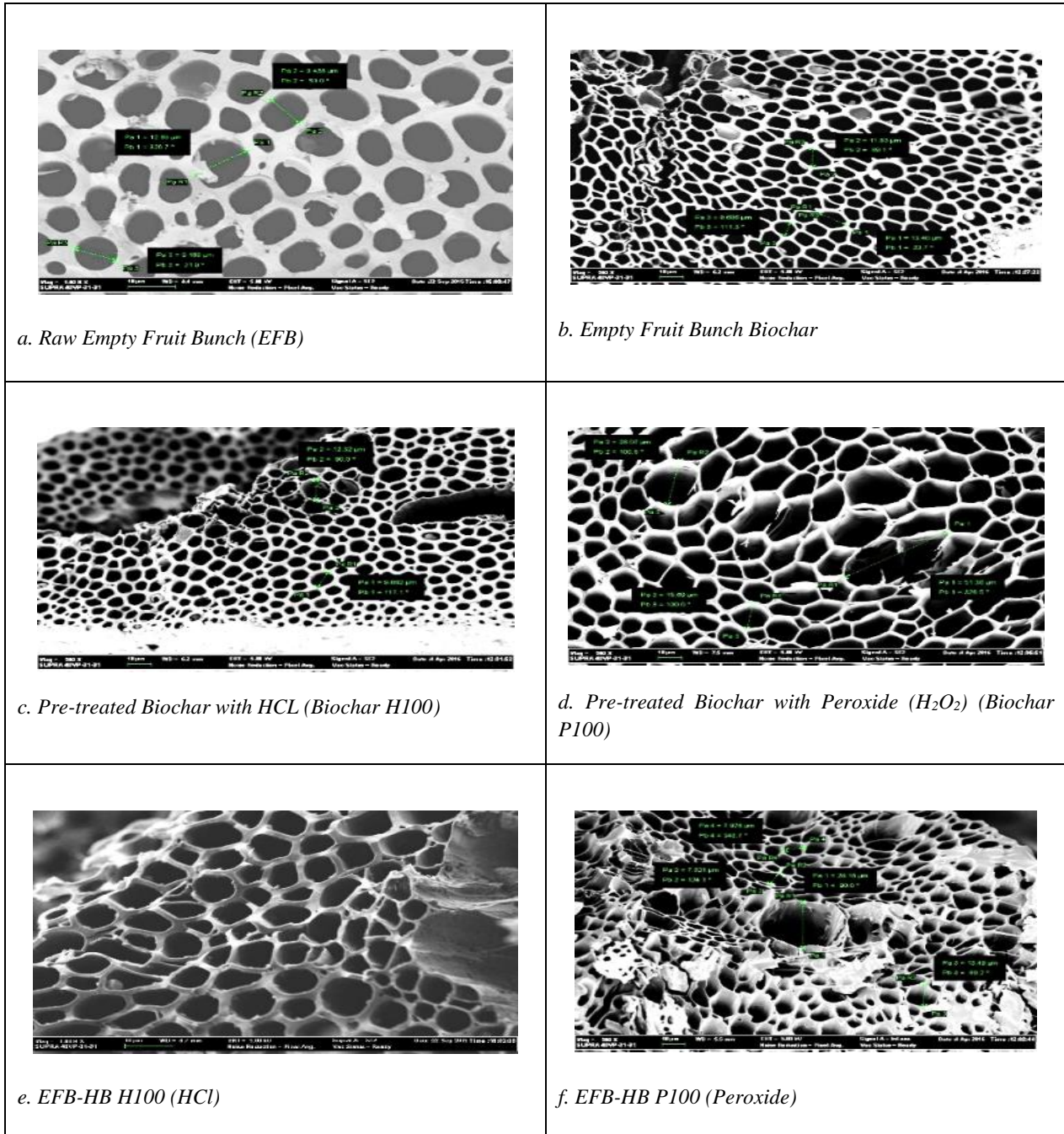


Table 1 BET surface area and porosity results

Material	BET surface area, m ² /g	Total pore volume, cm ³ /g	Average Pore Size, nm
Raw EFB	1.6061	0.001729	6.6628
Biochar	1.9431	0.005851	10.4459
Biochar H100	13.6074	0.009366	3.3589
Biochar P100	111.6225	0.045540	1.7544
EFB-HBC H100	1.2562	0.000951	3.0272
EFB-HBC P100	1.5997	0.000965	3.8381

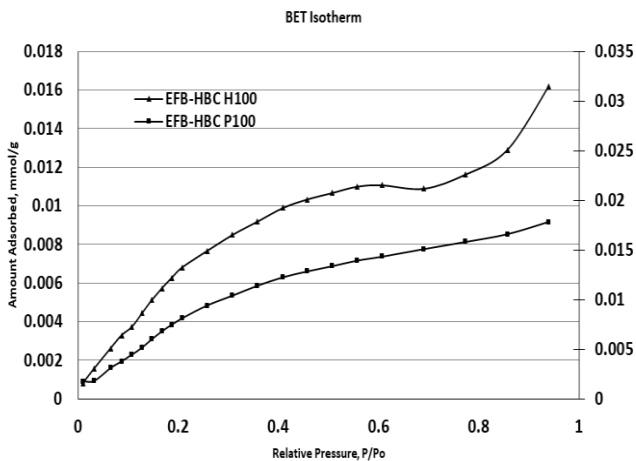


Figure 4 BET isotherm for HBCs

The BET surface area of EFB-HBCs was considered a low surface area. However, further studies on sorption performance will prove that EFB-HBC is a good adsorbent. The thermogravimetric analysis (TGA) curves for EFB-HBC H100 and EFB-HBC P100 are illustrated in Figure 5 and Figure 6, respectively. From the TG curve, it showed that EFB-HBC was almost completed at over 1000 °C the thermal decomposition indicates both HBCs was thermally stable. The first peak (25 °C < T < 135 °C) in DTG curve represented a mass loss mainly due to moisture evaporation [18]. DTG profile of EFB-HB H100 and EFB-HB P100 exhibited two peak temperatures around $T_{p, 1} = 300$ °C and $T_{p, 2} = 400$ °C. Meanwhile, the temperature around (200 °C to 400 °C) is mainly related to the decomposition of volatile matter such as cellulose, hemicelluloses, and some of the polymer from hydrogel polymerization [20]. The final peak at 950°C was represent the thermal degradation of carbon and the remaining curve is the ash content. Those three regions are in agreement with other researchers [13-15]. The proximate analysis results were provided in Table 2. It can be observed that the moisture content was decreasing from treated biochar (Biochar H100: 8.81 % and Biochar P100: 7.52 %) and became Hydrogel Biochar Composite (HBC) (EFB-HBC H100: 5.19 % and EFB-HBC P100: 3.39 %). After the polymerization process, the volatile matter has increased from the treated biochar (Biochar H100:10.99 % and Biochar P100: 8.08 %) and became (EFB-HBC H100:

25.85 % and EFB-HBC P100: 24.53 %). In addition, EFB-HBC H100 had higher carbon content at 30.97 % compared to EFB-HBC P100 at 21 %. The reason is that treated biochar by using H₂O₂ has oxidized some amount of carbon in the EFB biochar. Finally, the ash content of EFB-HBC P100 was higher with 50 % compared to EFB-HBC H100 with only 37.88 %.

Figure 7 shows the DSC curves for all samples (Raw EFB, EFB biochar, Biochar H100, Biochar P100, EFB-HBC H100, and EFB-HBC P100). As shown in Figure 7, DSC curve for raw EFB showed a high endothermic peak indicates the glass transition which exhibits enthalpy relaxation [21] band because of this phenomenon the raw EFB was classified as amorphous substances [22]. The similar results observed for biochars (Biochar, Biochar H100, and Biochar P100). However, glass transition temperature, from raw EFB pyrolysed to biochars were shifted to the right from $T_g = 68$ °C to $T_g = 89$ °C corresponding to increase the thermal transition. On the contrary, treated biochars (Biochar H100 and Biochar P100) are maintained at the same peak as biochars. This observations can be explained by the fact that the high amount of volatile matter was released during pyrolysis makes the material less reactive and the acid-treatment step eliminate the remaining volatile matter inside the biochars. Moreover, three consecutive endothermic curves which indicated substances that absorbed heat were observed for hydrogel biochars. Both of the hydrogel biochar composites (EHB-HBC H100 and EFB-HBC P100) have quite similar thermal behaviours and both of the HBCs have approximately the same glass transition temperature, T_g , around 86°C to 89°C. The other two curves were represented as the decomposition of substances. Additionally, the DSC curves also showing that both HBCs lose crystallization water in two steps at T_{m1} , 298°C and T_{m2} , 400°C and this is an agreement with Michalak et al. (2015) [23]. In addition, the presence of double endothermic peak concludes that HBCs is enantiotropic and polymorphic compound [24]. Polymorphism is a single substance that exhibits multiple different crystal structures, or, in other words, they have various melting phase transitions [25].

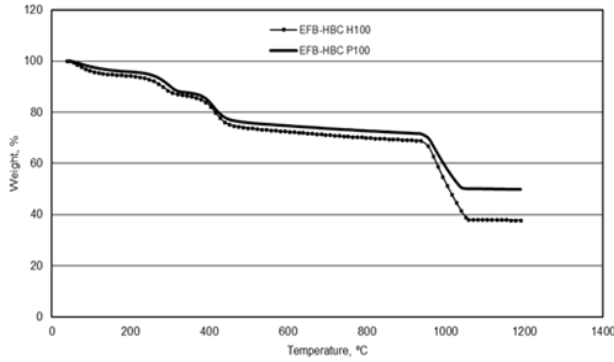


Figure 5 Thermogravimetric (TG) curve for EFB-HBC H100 and EFB-HBC P100

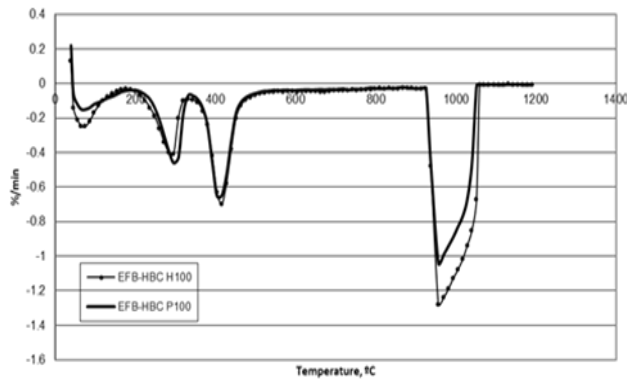


Figure 6 Derivative Thermogravimetric (DTG) curve for EFB-HBC H100 and EFB-HBC P100

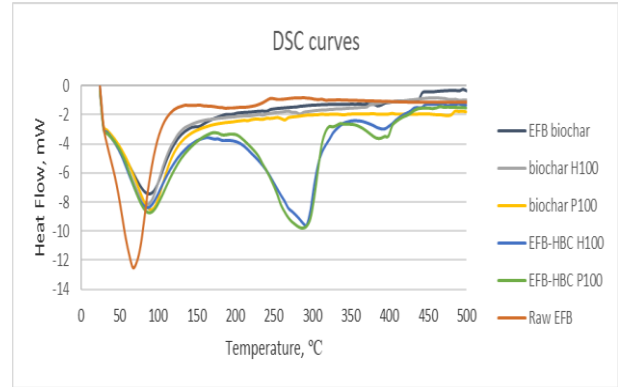


Figure 7 DSC curves study for Raw EFB, EFB biochar, Biochar H100, Biochar P100, EFB-HBC H100 and EFB-HBC P100

Table 2 Proximate analysis result for HBCs

Material	Moisture Content %	Volatile Content %	Carbon Content %	Ash Content %
Raw EFB	7.82	26.82	6.44	36.08
Biochar	7.28	11.61	41.81	39.26
Biochar H100	8.81	10.99	65.05	15.14
Biochar P100	7.52	8.08	47.76	36.93
EFB-HBC H100	5.19	25.85	30.97	37.88
EFB-HBC P100	3.39	24.53	21.00	50.00

Figure 8 shows the FTIR spectrum for the studied samples. The spectrum of raw EFB showed a broad characteristic peak at 3259.38 cm^{-1} , which indicates the presence of O–H stretching. The same results similar to Claoston et al., (2014) which recognized the stretching functional group of a hydrogen-bonded hydroxyl group (O–H), indicative of the presence of phenols and alcohols. During biochar production via pyrolysis, the O–H groups were diminished because of the mass loss during thermal decomposition [27]. The same results were seen for biochar treated by HCl

(Biochar H100) due to diminishing of volatile matter during the washing pre-treatment. The stretching vibration of O=C=O (CO_2) with a wavelength of 2352.1 cm^{-1} was observed. The presence of CO_2 in EFB biochar was from the pyrolysis process which has generally produced gaseous products rich in CO_2 . Moreover, CO_2 was removed and diminish after being treated with HCl (Biochar H100) and this is clearly seen in the FTIR spectrum for Biochar H100 [16]. According to Asim et al., (2015), peaks around 1700 cm^{-1} indicated the presence of holocellulose and lignin

which were shown for Biochar H100 and EFB-HBC H100 of wavelength 1737.80 cm^{-1} and 1736.23 cm^{-1} respectively [26]. This means that the formation of hydrogel biochar composite did not destroy the lignin the important to the structure of HBC. For EFB biochar and EFB-HBC H100, they have the same bending vibration at curve 1366 cm^{-1} represented the existence of the C-H (alkane) group and the same stretching vibration on 1216 cm^{-1} showed the existence of C-O group. After the polymerization process EFB biochar becoming the hydrogel biochar composite (HBC), there were changes in functional the group with the addition of C=C stretching and amine C-N stretching on 1602 cm^{-1} and 1081 cm^{-1} respectively. This is because of the addition Acrylamide (AAm) as monomer, and N,N'-methylenebisacrylamide (MBA) as cross-linker in the polymerization process.

Relatively, Figure 8 and 9 show the FTIR spectrum for Raw EFB, EFB-HBC P100, Biochar P100, and EFB biochar. The peaks of EFB-HBC P100 showed that there was low transmittance, and hence, a large absorption ability as compared to EFB-HBC H100. As can be seen in this figure, the biochar H100 had the same pattern or spectrum with peaks around 1700 cm^{-1} indicating the presence of holocellulose and lignin, 1366 cm^{-1} existing in the C-H (alkane) group and peaks around 1216 cm^{-1} showing the existence of the C-O group. In addition, CO_2 was diminished after treatment with H_2O_2 (Biochar P100). After polymerization becoming EFB-HBC P100, peaks were around 3197.41 cm^{-1} which were represented as existence phenols and alcohols in the structure. The same with EFB-HBC H100, after the polymerization process, they were changes in the functional group with the addition of C=C stretching and primary amine C-N stretching on 1651 cm^{-1} and 1082 cm^{-1} respectively.

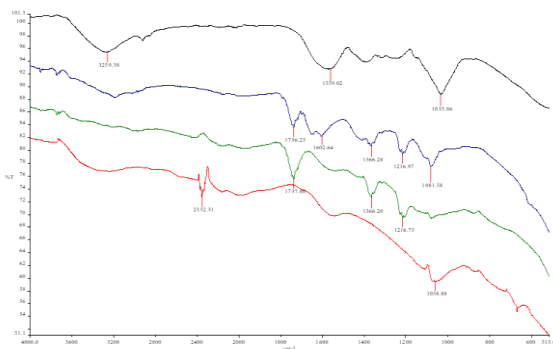


Figure 8 FTIR spectrum (from the top: raw EFB, EFB-HBC H100, biochar H100, EFB biochar)

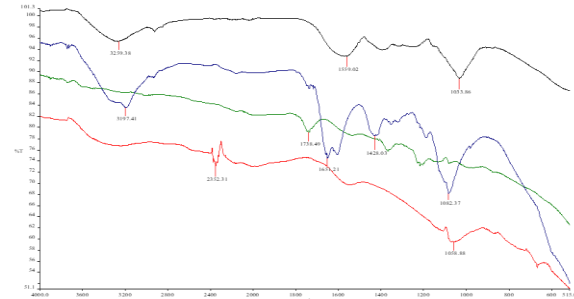


Figure 9 FTIR spectrum (from the top: raw EFB, EFB-HBC P100, biochar P100, EFB biochar)

3.2 Adsorption Test

Sorption performance of H_2S gas by EFB-HBC has shown in the form of a breakthrough curve where the curves were plotted by C_f/C_i against time. As shown in Figure 10, increasing the bed height increases the breakthrough time and sorption capacity. The increasing trend was due to the increase of available binding sites for the adsorption. The same pattern showed for increasing the breakthrough time with bed height for the wet granule EFB-HBC, dry fine size EFB-HBC and wet fine size EFB-HBC. Figure 12 shows the comparison of breakthrough behavior between the Granule size of EFB-HBC in dry and wet conditions. It showed that the breakthrough time for wet granule size of EFB-HBC in adsorption of Hydrogen Sulphide is longer compared to the breakthrough time for dry granule size. The longest breakthrough time was 6 minutes for Wet Granule EFB-HBC at the highest bed height of 6 inches. Meanwhile, the breakthrough time was 2.33 minutes for Dry Granule EFB-HBC. Based on the breakthrough time from the effects of bed height adsorption performance test it showed that the presence of water to EFB-HBC has improved the adsorption performance, especially in the fine size EFB-HBC. As shown in Figure 13, the fine size of EFB-HBC in wet conditions had significant results with the longest breakthrough time of 85 minutes at 6 inches of bed height compared to the dry condition of only 30 minutes. This is due to the smaller the sorbent size, the higher the surface area. The wet fine size of EFB-HBC was observed to have a sponge-like characteristic and had a strong attraction to H_2S because of the water presence. The bar chart in Figure 11 shows the adsorption capacity (mg/g) observed in the adsorption performance of H_2S . It showed that increasing the bed height for all samples will increase the adsorption capacity. The presence of water to granule size or fine size of EFB-HBC in adsorbing H_2S showed significant results. The most powerful sample was the fine EFB-HBC in the wet condition which had 102 mg/g of adsorption capacity compared to granule size (wet and dry) and dries fine size of EFB-HBC as shown in Figure 11.

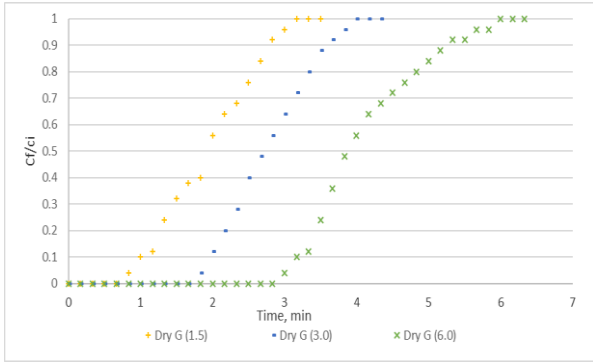


Figure 10 Effect of bed height on the breakthrough profile for sorption of H₂S

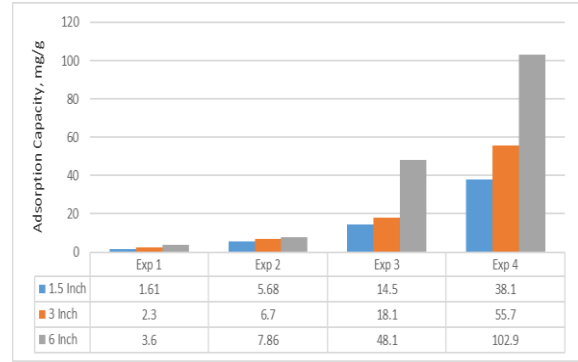
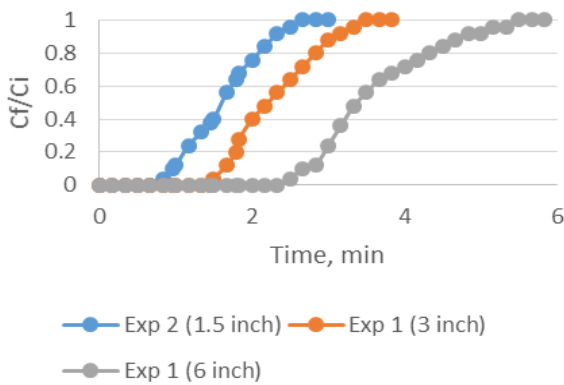
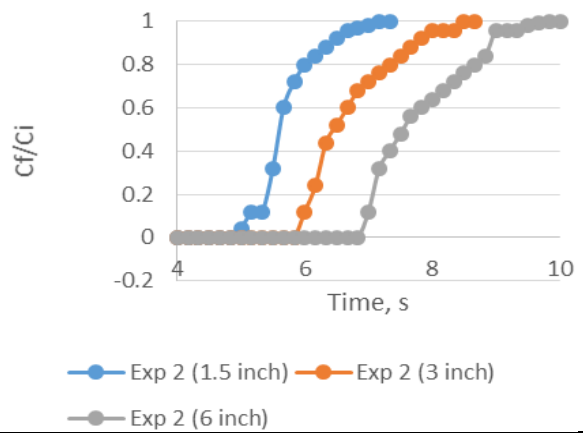


Figure 11 Comparison study for adsorption capacity

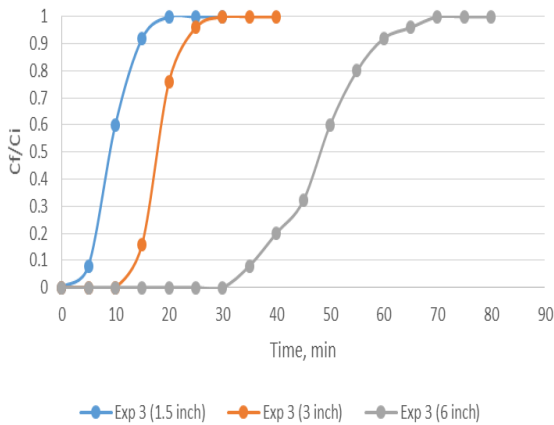


Bed Height (inch)	Breakthrough Time (min)
1.5	0.67
3	1.46
6	2.33

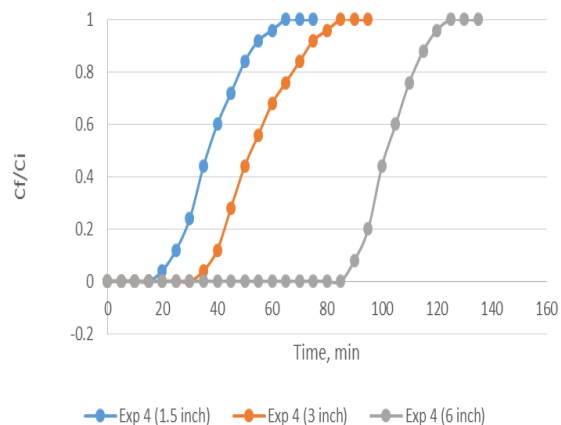


Bed Height (inch)	Breakthrough Time (min)
1.5	4
3	5
6	6

Figure 12 Breakthrough behaviour for granule EFB-HBC in dry condition and wet condition



Bed Height (inch)	Breakthrough Time (min)
1.5	5
3.0	10
6.0	30



Bed Height (inch)	Breakthrough Time (min)
1.5	15
3.0	30
6.0	85

Figure 13 Breakthrough behaviour for fine EFB-HBC in dry condition and wet condition

4. CONCLUSION

In conclusion, based on characterization analysis, EFB-HBC P100 was selected as adsorbent based on characterization results. It is believed have a good characteristic and become versatile adsorbent. For adsorbent performance, the higher bed height, more H₂S adsorbed. This hypothesis can be applied to all conditions (granule, fine, wet, dry). The breakthrough capacity showed increasing pattern by increasing bed height because of more active site available as amount of adsorbent used increases. Meanwhile, the effect of adsorbent size on breakthrough curve showed that, the smaller size of EFB-HBC has greater adsorption capacity due to increases of surface area. The most succeed adsorption performance is when the presence of water on the EFB-HBC which swelled and open more active site of adsorbent and this phenomenon can be assumed because of the reaction occurred in between water and H₂S which encouraged the adsorption capacity. In future, EFB-HBC will widely apply in adsorption industries, then, comprehensive regeneration study will strengthen the ability of EFB-HBC in order to achieve the most economical adsorbent in the world, which can be regenerate the adsorbent to use for long terms.

ACKNOWLEDGMENT

The authors would like to thank Universiti Teknologi MARA (UiTM) and Ministry of Higher Education Malaysia (MOHE) for the financial supports. The research was conducted at the Faculty of Chemical Engineering, UiTM under the support of REI grant (600-IRMI/REI 5/3 (006/2019)).

REFERENCES

- [1] Dennis Darylmp and Bryan Petrincec, "New Process for H₂S Management Now Commercially Available," Tartan Engineering, Canada, pp. 2–4, 2007.
- [2] West Texas Safety Training Centre, "H₂S in the Oilfield – Fact Sheet," West Texas Safety Training Centre, Texas, pp. 1–3, Feb-2011.
- [3] M. T. M. N. and R. M. Muhammad Afif Ariffin, Wan Mohd Faizal Wan Mahmood, "Australian Journal of Basic and Applied Sciences Potential of Oil Palm Empty Fruit Bunch (EFB) Biochar from Gasification Process," *Aust. J. Basic Appl. Sci.*, vol. 8, no. 19, pp. 149–152, 2014. ISSN:1991-8178
- [4] E. Onoja, "Oil Palm (*Elaeis guineensis*) Biomass in Malaysia : The Present and Future Oil Palm (*Elaeis guineensis*) Biomass in Malaysia : The Present and Future Prospects," *Waste and Biomass Valorization*, vol. 0, no. 0, p. 0, 2018. DOI: <https://doi.org/10.1007/s12649-018-0258-1>
- [5] E. Antunes, M. V. Jacob, G. Brodie, and P. A. Schneider, "Silver removal from aqueous solution by biochar produced from biosolids via microwave pyrolysis," *J. Environ. Manage.*, vol. 203, pp. 264–272, 2017. DOI: <https://doi.org/10.1016/j.jenvman.2017.07.071>
- [6] A. R. Hibbins, P. Kumar, Y. E. Choonara, P. P. D. Kondiah, T. Marimuthu, L. C. du Toit, and V. Pillay, "Design of a versatile pH-responsive hydrogel for potential oral delivery of gastric-sensitive bioactives," *Polymers (Basel)*, vol. 9, no. 10, 2017. DOI: <https://doi.org/10.3390/polym9100474>
- [7] O. Okay, "General Properties of Hydrogels," *Hydrogel Sensors and Actuators*, vol. 6, pp. 1–15, 2010. DOI: https://doi.org/10.1007/978-3-540-75645-3_1
- [8] F. Z. Abas and F. Nasir Ani, "Comparing Characteristics of Oil Palm Biochar Using Conventional and Microwave Heating," *J. Teknol.*, vol. 3, pp. 33–37, 2014. DOI: <https://doi.org/10.11113/jt.v68.2926>
- [9] Y. Fernández, A. Arenillas, and J. Á. Menéndez, "Microwave heating applied to pyrolysis," *Microw. Heat. Appl. to Pyrolysis*, pp. 723–752, 2011. DOI: <https://doi.org/10.5772/13548>
- [10] Zakiuddin Januri, Rahman, N. Abdul, Idris, S. Shawalliah, S. Matali, and S. F. A. Manaf, "MICROWAVE ASSISTED PYROLYSIS (MAP) OF AUTOMOTIVE PAINT SLUDGE (APS)," *J. Teknol.*, vol. 5, no. 8, pp. 103–109, 2014. DOI: <https://doi.org/10.11113/jt.v75.5202>
- [11] O. Okay, "General Properties of Hydrogels," *Hydrogel Sensors and Actuators*, vol. 6, pp. 1–15, 2010. DOI: https://doi.org/10.1007/978-3-540-75645-3_1
- [12] N. Karakoyun, S. Kubilay, N. Aktas, O. Turhan, M. Kasimoglu, S. Yilmaz, and N. Sahiner, "Hydrogel-Biochar composites for effective organic contaminant removal from aqueous media," *Desalination*, vol. 280, no. 1–3, pp. 319–325, 2011. DOI: <https://doi.org/10.1016/j.desal.2011.07.014>
- [13] N. H. Meri, A. B. Alias, N. Talib, Z. A. Rashid, W. A. Wan, and A. K. Ghani, 'Effect of chemical washing pre-treatment of empty fruit bunch (EFB) biochar on characterization of hydrogel biochar composite as bioadsorbent', in *IOP Conference Series: Materials Science and Engineering*, 2018, vol. 358, no. 1, p. 12018. DOI: <https://doi.org/10.1088/1757-899X/358/1/012018>
- [14] B. Kusuktham, J. Prasertgul, and P. Srinun, 'Morphology and Property of Calcium Silicate Encapsulated with Alginate Beads', *Silicon*, vol. 6, no. 3,

pp. 191–197, 2014. DOI: <https://doi.org/10.1007/s12633-013-9173-z>

[15] M. A. F. Supian, K. N. M. Amin, S. S. Jamari, and S. Mohamad, ‘Production of cellulose nanofiber (CNF) from empty fruit bunch (EFB) via mechanical method’, *J. Environ. Chem. Eng.*, vol. 8, no. 1, p. 103024, 2020. DOI: <https://doi.org/10.1016/j.jece.2019.103024>

[16] E. H. Novotny, ‘Properties of Pyrolysis Residues Produced and their Utility as Biochars,’ p. 227248, 2013. DOI: <https://doi.org/10.1007/s11157-020-09523-3>

[17] Y. Liu, Z. He, and M. Uchimiya, ‘Comparison of Biochar Formation from Various Agricultural By-Products Using FTIR Spectroscopy,’ vol. 9, no. 4, pp. 246–253, 2015. DOI: <https://doi.org/10.5539/mas.v9n4p246>

[18] A. J. White and A. J. White, ‘Development of an Activated Carbon from Anaerobic Digestion By-Product to Remove Hydrogen Sulfide from Biogas by Development of an Activated Carbon from Anaerobic Digestion By-Product to Remove Hydrogen Sulfide from Biogas,’ 2010. Retrieved from: <http://hdl.handle.net/1807/33707>

[19] P. E. Dr. Samy Sadaka, P.E., ‘Pyrolysis,’ Iowa State University, 2008. Retrieved from: <https://www.yumpu.com/s/VvJ0b8W2yb8pHYt4>

[20] A. Diaz, J. Le Toullec, A. Blandino, I. De Ory, and I. Caro, ‘Pretreatment of rice hulls with alkaline peroxide to enhance enzyme hydrolysis for ethanol production,’ *Chem. Eng. Trans.*, vol. 32, pp. 949–954, 2013. DOI: <https://doi.org/10.3303/CET1332159>

[21] M. Rafatullah, O. Sulaiman, R. Hashim, and A. Ahmad, ‘Adsorption of methylene blue on low-cost adsorbents: A review,’ *J. Hazard. Mater.*, vol. 177, no. 1–3, pp. 70–80, 2010. DOI: <https://doi.org/10.1016/j.jhazmat.2009.12.047>

[22] Z. A. Alothman, ‘A review: Fundamental aspects of silicate mesoporous materials,’ *Materials (Basel)*, vol. 5, no. 12, pp. 2874–2902, 2012. DOI: <https://doi.org/10.3390/ma5122874>

[23] S. S. Idris, N. A. Rahman, K. Ismail, A. B. Alias, Z. A. Rashid, and M. J. Aris, ‘Investigation on thermochemical behaviour of low rank Malaysian coal, oil palm biomass and their blends during pyrolysis via thermogravimetric analysis (TGA),’ *Bioresour. Technol.*, vol. 101, no. 12, pp. 4584–4592, 2010. DOI: <https://doi.org/10.1016/j.biortech.2010.01.059>

[24] M. Toledo, ‘Thermal Analysis of Polymers Selected Applications,’ Mettler Toledo, pp. 1–40, 2008. Retrieved from: [https://www.mt.com/dam/Analytical/ThermalAnalysis/TA-](https://www.mt.com/dam/Analytical/ThermalAnalysis/TA-PDF/Part%20of%20Polymers-Selected%20Applications.pdf)

[PDF/Part%20of%20Polymers-Selected%20Applications.pdf](https://www.mt.com/dam/Analytical/ThermalAnalysis/TA-PDF/Part%20of%20Polymers-Selected%20Applications.pdf)

[25] J. Shawe, R. Riesen, J. Widmann, and M. Schubnell, ‘UserCom,’ Mettler Toledo, pp. 1–28, 2000. Retrieved from: <https://www.mt.com/my/en/home/library/collections/lab-analytical-instruments/AnaChemUserCom.html>

[26] O. Michalak, M. Łaszcz, K. Jateczak, A. Witkowska, I. Bujak, A. Groman, and M. Cybulski, ‘New Polymorphic Forms of Pemetrexed Diacid and Their Use for the Preparation of Pharmaceutically Pure Amorphous and Hemipentahydrate Forms of Pemetrexed Disodium,’ *Molecules*, vol. 20, no. 8, pp. 13814–13829, 2015. DOI: <https://doi.org/10.3390/molecules200813814>

[27] C. Moriwaki, G. L. Costa, C. N. Ferracini, F. F. De Moraes, G. M. Zanin, E. A. G. Pineda, and G. Matioli, ‘Enhancement of solubility of albendazole by complexation with ??-cyclodextrin,’ *Brazilian J. Chem. Eng.*, vol. 25, no. 2, pp. 255–267, 2008. DOI: <https://doi.org/10.1590/S0104-66322008000200005>

[28] Y. Namatame and H. Sato, ‘Evaluation of polymorphic forms by powder X-ray diffraction and thermal analysis methods,’ *Rigaku J.*, vol. 29, no. 3, pp. 8–15, 2013. Retrieved from: <https://pdfs.semanticscholar.org/c1cb/7e09765d6679216ad90ac815e544c9b64cb9.pdf>

[29] M. Asim, K. Abdan, M. Jawaid, M. Nasir, Z. Dashtizadeh, M. R. Ishak, and M. E. Hoque, ‘A Review on Pineapple Leaves Fibre and Its Composites,’ *Int. J. Polym. Sci.*, vol. 2015, pp. 1–17, 2015. DOI: <https://doi.org/10.1155/2015/950567>

[30] N. Claoston, A. Samsuri, M. Ahmad Husni, and M. Mohd Amran, ‘Effects of pyrolysis temperature on the physicochemical properties of empty fruit bunch and rice husk biochars,’ *Waste Manag. Res.*, vol. 32, no. 4, pp. 331–9, 2014. DOI: <https://doi.org/10.1177/0734242X14525822>